

0203

Measuring transmembrane water exchange in rat brain cortical cells in normal and pathological conditions

Ruiliang Bai¹, Charles S. Springer, Jr.², Dietmar Plenz³, and Peter Basser¹

¹Section on Quantitative Imaging and Tissue Sciences, DIBGI, NICHD, National Institutes of Health, Bethesda, MD, United States, ²Advanced Imaging Research Center, Oregon Health & Science University, Portland, OR, United States, ³Section on Critical Brain Dynamics, LSN, NIMH, National Institutes of Health, Bethesda, MD, United States

Synopsis

Knowledge of transmembrane water exchange kinetics is invaluable for the correct interpretation of many MRI experiments, e.g., DCE-MRI, diffusion MRI, etc. Here we quantitatively studied the transmembrane water exchange in organotypic cultures from rat brain cortex with an MR relaxation contrast agent. In normal states, we determined the equilibrium cellular water efflux rate constant [k_{i0}] is $2.15 (\pm 1.28) \text{ s}^{-1}$ at $34 (\pm 1) ^\circ\text{C}$. In the likely cell-swollen state induced by Ouabain perfusion, we, for the first time, quantitatively measured a global increase of the intracellular volume fraction ($\sim 104\%$) together and a large decrease of k_{i0} ($\sim 64\%$).

Purpose

Water in the intra- and extracellular spaces is in steady-state exchange. Knowledge of the exchange kinetics is invaluable for correctly interpreting findings obtained in many MRI experiments, e.g., DCE-MRI,¹ diffusion MRI,^{2,3} etc. Moreover, the exchange rate constant itself might provide important physiological and pathological information, e.g., about metabolic activity.⁴ Dominating over the passive pathways based on diffusion across membranes, transmembrane water cycling enjoys a metabolically active pathway via the $\text{Na}^+\text{-K}^+\text{-ATPase}$ (NKA) pump, which is essential for all mammalian cells and is primarily responsible for maintaining the K^+ and Na^+ gradient *in vivo*.^{1,5} Dysfunction of the NKA pump is also reported involved in many pathological processes, like cerebral ischemia, etc.⁶ Thus, the determination of transmembrane water exchange kinetics when the NKA-pump is blocked will also provide crucial biological information.

Methods

We studied organotypic tissue cultures from rat brain cortex using a novel multimodality imaging test bed with simultaneous intracellular calcium fluorescence imaging and MR acquisition capabilities.^{7,8} The organotypic cortical cultures were kept perfused with artificial CSF (ACSF) at a constant temperature $34.0 (\pm 1.0) ^\circ\text{C}$. Longitudinal MR relaxometry with an extracellular gadolinium-based MR relaxation contrast agent (CA), Gadoteridol (Prohance (PH)), was used to distinguish intracellular and extracellular water compartments by increasing the extracellular water's longitudinal relaxation rate constant. A saturation-recovery MR sequence with 21 recovery times was used to measure sample R_1 values at three different PH concentrations: 0, 2.5 and 5.0 mM. Data were further analyzed with a two-sites-exchange (2SX) model⁴ to determine the transmembrane water exchange kinetics with the following parameters: f_i – intracellular water molar fraction; k_{i0} – the equilibrium cellular water efflux rate constant [where $\tau_i [= 1/k_{i0}]$ is the intracellular water residence time]; and R_{1i} – the intracellular water R_1 . NKA pump blockage was induced by adding 1mM Ouabain (an NKA pump inhibitor) into the perfusing medium.

Results

Evidence of Exchange. In **Figure 1**, the R_1 data from ACSF is fit well by single-exponential functions at the three PH concentrations. The organotypic culture R_1 data were also fit well by a single-exponential function when $[\text{PH}] = 0 \text{ mM}$, but required at least a bi-exponential function at $[\text{PH}] = 2.5$ and 5.0 mM . A significant decrease of the apparent fraction of the signal (f_{sm}) with a small apparent R_1 ($R_{1,sm}$) from $[\text{PH}] = 2.5$ to 5 mM was observed ($p < 0.005$, **Figure 2**). This demonstrated the presence of transmembrane proton exchange. **2SX Model.** The 2SX model was applied to the data obtained on a single concentration ($[\text{PH}] = 5.0 \text{ mM}$) with constraints obtained from single-exponential fit on the data collected at $[\text{PH}] = 0 \text{ mM}$. The 2SX model well fit the R_1 data without any systematic bias in the residuals and reported the intracellular water residence time

Figures

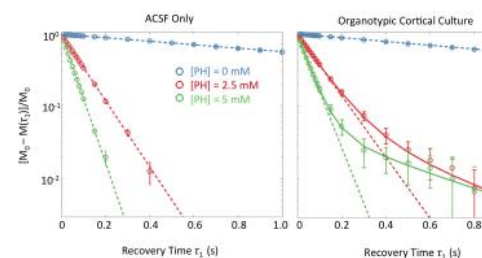


Figure 1. The averaged saturation recovery data from ACSF only (left, $n = 6$) and organotypic cortical cultures (right, $n = 13$) at three $[\text{PH}]$ values, in which the dashed and continuous lines are the fitting results from single-exponential and empirical bi-exponential models, respectively. The errorbars represent the standard deviation on each measurement. $M(\tau_1)$ is the magnetization at recovery time τ_1 and M_0 is the equilibrium magnetization.

ACSF ($n = 6$)			
$[\text{PH}]$ (mM)	0	2.5	5
R_1 (s^{-1})	$0.55 (\pm 0.01)$	$10.40 (\pm 0.12)$	$20.23 (\pm 0.17)$
Organotypic Cortical Culture ($n = 13$)			
$[\text{PH}]$ (mM)	0	2.5	5
f_{sm} (%)	N.A	$9.78 (\pm 1.01)$	$6.82 (\pm 0.60)$
$R_{1,sm}$ (s^{-1})	$0.60 (\pm 0.01)$	$2.97 (\pm 0.21)$	$2.92 (\pm 0.27)$
$R_{1,i}$ (s^{-1})		$10.62 (\pm 0.15)$	$19.76 (\pm 0.25)$

R_1 – apparent relaxation rate constant in the single-exponential function
 $R_{1,sm}$ and $R_{1,i}$ – small and large apparent relaxation rate constants in the bi-exponential function
 f_{sm} – apparent intensity fraction of the signal with $R_{1,sm}$ in the bi-exponential function

Figure 2. Results of the single- and empirical bi-exponential fittings of saturation recovery data from ACSF only, and ACSF with organotypic cultures at three different $[\text{PH}]$ values

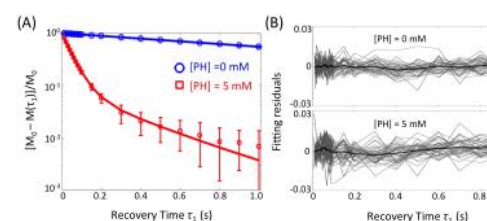


Figure 3. The results (A) and residuals (B) of 2SX fittings of the saturation recovery data from organotypic cortical cultures ($n = 45$) at $[\text{PH}] = 0 \text{ mM}$ and 5 mM .

$M(\tau_1)$ is the magnetization at

~465 (\pm 276) ms (**Figure 3** and **Figure 4**). **NKA Blockage.** As shown in **Figure 5**, the intracellular calcium content increased and reached its maximum around ~10 min after starting Ouabain perfusion, and then slowly decreased while Ouabain perfusion continued. The f_i values showed almost synchronous behavior – it increased and reached its maximum (from 7.1% to 14.4%) around ~ 20 min after starting Ouabain perfusion. On the other hand, k_{io} showed opposite changes – significantly decreasing (from 4.0 s^{-1} to 1.4 s^{-1}) after 20-min Ouabain perfusion. The R_{1i} also showed small decrease (from 1.4 s^{-1} to 1.2 s^{-1}).

Discussion

Brain tissue transmembrane water exchange has been measured only with intracerebroventricular Gd(DTPA) $^{2-}$ infusion into rat brain; $k_{io} = 1.81 (\pm 0.89) s^{-1}$.⁹ Our k_{io} value measured under normal conditions agrees with this. This information will be useful to model and interpret many MRI experiments, *e.g.*, time-series analysis in DCE-MRI, inter-compartment exchange effects on diffusion MRI, *etc.* Ouabain has been used to presumably induce cell swelling by blocking the NKA pump for decades,¹⁰ but this phenomenon has never been directly characterized by MR. This study, for the first time, quantitatively measured a global f_i increase during NKA blockage. If the mean cellular volume is $\langle V \rangle$: $f_i = \rho \langle V \rangle f_w / (1 - \rho \langle V \rangle f_M)$; where ρ is the cell number density, f_w is the volume fraction accessible to mobile aqueous solutes, and $f_M = 1 - f_w$. $R_{1i} \sim \langle V \rangle^{-1}$. Interestingly, a large decrease of the transmembrane water exchange is also observed during NKA blockage. In addition, the simultaneous cellular calcium uptake also indicates the calcium might play an important role in this pathological process.¹¹ These new findings may provide important clues to not only for the interpretation of some MRI biomarkers on disease, but also to understand some essential physiological processes underlying these diseases, *e.g.*, in cerebral ischemia.

Acknowledgements

This work was supported by the Intramural Research Program (IRP) of the *Eunice Kennedy Shriver* National Institute of Child Health and Human Development, National Institutes of Health. Charles S. Springer, Jr. is supported by the National Institutes of Health under Awards No. UO1-CA154602 and R44-CA180425

References

- Springer CS, Li X, Tudorica LA, et al. Intratumor mapping of intracellular water lifetime: metabolic images of breast cancer? *NMR Biomed.* 2014; 27:760-773.
- Nilsson M, Lätt J, Nordh E, Wirestam R, Ståhlberg F, Brockstedt S. On the effects of a varied diffusion time in vivo: is the diffusion in white matter restricted? *Magn Reson Imaging.* 2009;27(2):176-187.
- Lee J-HH, Springer CS. Effects of equilibrium exchange on diffusion-weighted NMR signals: The diffusigraphic “shutter-speed.” *Magn Reson Med.* 2003;49(3):450-458.
- Zhang Y, Poirier-Quinot M, Springer CS, Balschi JA. Active Trans-Plasma Membrane Water Cycling in Yeast Is Revealed by NMR. *Biophys J.* 2011;101(11):2833-2842.
- Zhang Y, Balschi JA. Water Exchange Kinetics in the Isolated Heart Correlate with Na⁺/K⁺ ATPase Activity: Potentially High Saptiotemporal Resolution. *Proc Intl Soc Mag Reson Med.* 2013;1(21):4045.
- Rudolphi KA, Schubert P. Adenosine and Brain Ischemia. In: Adenosine and Adenine Nucleotides: From Molecular Biology to Integrative Physiology. Boston, MA: Springer US; 1995:391-397.
- Bai R, Klaus A, Bellay T, et al. Simultaneous calcium fluorescence imaging and MR of ex vivo organotypic cortical cultures?: a new test bed for functional MRI. *NMR Biomed.* 2015;28:1726-1738.
- Bai R, Stewart C V, Plenz D, Bassar PJ. Assessing the sensitivity of diffusion MRI to detect neuronal activity directly. *Proc Natl Acad Sci U S A.* 2016;113(12):E1728-1737.
- Quirk JD, Bretthorst GL, Duong TQ, et al. Equilibrium water exchange between the intra- and extracellular spaces of mammalian brain. *Magn Reson Med.* 2003;50(3):493-499.

recovery time τ_1 and M_0 is the equilibrium magnetization. In (A), the errorbars represent the standard deviation on each measurement. In (B), the light gray curves are residuals of 2SX fitting of each sample and the black curve is the average of all samples.

2SX model on organotypic cortical cultures (n = 45)				
Parameters	f_i (%)	k_{io} (s^{-1})	τ_1 (ms)	R_{1i} (s^{-1})
Mean \pm SEM	7.21 (\pm 2.22)	2.15 (\pm 1.28)	465 (\pm 276)	1.47 (\pm 0.43)

f_i – intracellular water molar fraction
 k_{io} – equilibrium cellular water efflux rate constant
 τ_1 – intracellular water residence time
 R_{1i} – intracellular water proton R_1 value

Figure 4. Results of 2SX model fitting on the organotypic cultures.

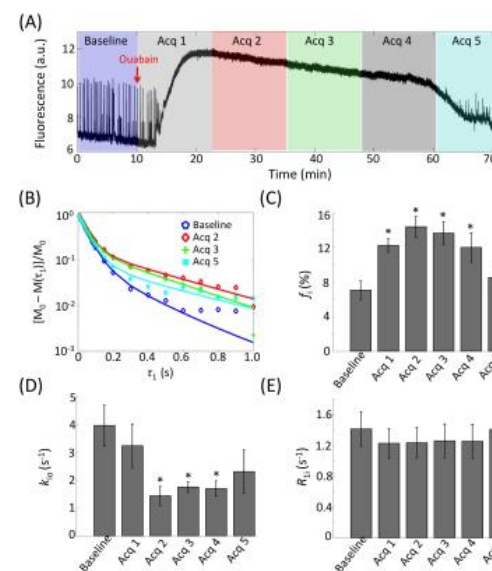


Figure 5. Ouabain experiment. (A) A representative intracellular calcium fluorescence trace during the introduction of 1 mM Ouabain. The different color regions represent the times of

10. Buckley DL, Bui JD, Phillips MI, et al. The effect of ouabain on water diffusion in the rat hippocampal slice measured by high resolution NMR imaging. *Magn Reson Med.* 1999;41(1):137-142.

11. Dirnagl U, Iadecola C, Moskowitz MA. Pathobiology of ischaemic stroke: an integrated view. *Trends Neurosci.* 1999;22(9):391-397.

each NMR acquisitions. (B) The averaged saturation recovery data ($n = 6$) at various time points; the continuous curves result from 2SX data fitting. (C-E) the statistical results of intracellular volume fraction (C), cellular water efflux rate constant (D), and intracellular water R_1 (E). * $p < 0.05$ with paired Student's t test compared with baseline values.